JOURNAL OF SOLID STATE CHEMISTRY 95, 21–28 (1991)

Magnetic and Electronic Transport Properties of the Monophosphate Tungsten Bronze $(PO_2)_4(WO_3)_{2m}$, $m = 2$

Z. S. TEWELDEMEDHIN, K. V. RAMANUJACHARY, AND M. GREENBLATT*

Department of Chemistry, Rutgers, The State University of New Jersey, Piscataway, New Jersey 08855

Received March 29, 1991; in revised form June 10, 1991

Large plate-like dark-brown crystals of monophosphate tungsten bronze $(PO_2)_4(WO_3)_{2m}$, $m = 2$ or PWO_5 were prepared by reacting stoichiometric mixtures of P_2O_5, WO_3, and W at 1200°C. The temperature dependence of electrical resistivity along each of the three unique crystallographic axes of a single crystal shows semiconducting behavior down to 50 K with an activation energy of ~0.084 eV. The room temperature resistivitity along the direction of corner sharing WO_6 octahedra is 5×10^{-3} $\Omega \cdot$ cm and about one to two orders of magnitude lower than along other unique directions, which implies quasi one-dimensional behavior. The magnetization study made on a batch of crystals in the temperature range of 2 to 300 K is indicative of antiferromagnetic ordering with a maximum at 15 K. An earlier theoretical study on the band electronic structure of $(PO_2)_4(WO_3)_4$ predicted both localized and delocalized electrons in narrow and dispersive bands, respectively. The observed magnetic moment of PWO_5 is consistent with the theoretical prediction, but the observed semiconductivity behavior is not. The difference in the observed electronic transport properties of PWO_5 from that of theoretically predicted behavior, as well as the anomalous magnetic and transport properties compared to the higher members of the series of the monophosphate tungsten bronzes $\{(PO_2)_4(WO_3)_{2m}, m = 4, 6\}$, is discussed in terms of the unique structure of PWO_5.

I. Introduction

Oxides that exhibit quasi low-dimensional transport properties have been the subject of intense investigation in recent years, because of their unusual magnetic and electronic transport properties. One such class of compounds that belong to this group of oxides is the phosphate tungsten bronzes. Single crystal studies made on some of these compounds show quasi low-dimensional transport properties and charge density wave (CDW) electronic instabilities, which are also supported by theoretical studies of the band electronic structure (*1–7*). One series in this class of bronzes is the monophosphate tungsten bronze (MPTB): $(PO_2)_4(WO_3)_{2m}$ (*8–14*) and $A_x(PO_2)_4(WO_3)_{2m}$ (*15–20*). The structure of the MPTB is generally built up of ReO_3-type slabs of WO_6 octahedra connected by PO_4 tetrahedra resulting in pentagonal, or hexagonal tunnels that can accommodate the alkali metal ions. So far, the electrical and magnetic properties of two compounds of the monophosphate tungsten bronzes with pentagonal tunnels ($MPTB_p$): $P_4W_{12}O_{44}$ ($m = 6$) (*4*) and $P_4W_8O_{32}$ ($m = 4$) (*21*) have been studied. $P_4W_{12}O_{44}$ shows anisotropy and anomalies in the electrical resistivity and magnetic susceptibility at low temperatures (*4*). To understand the origin of these anomalies,

0022-4596/91 $3.00

Whangbo and co-workers have carried out theoretical studies on the band electronic structure of the compound using tight-binding band calculations (*4*). These studies showed the nesting of one- and two-dimensional Fermi surfaces for $P_4W_{12}O_{44}$, which explains the observed quasi two-dimensional metallic property and associated electronic instability. Furthermore, these calculations have suggested that all related MPTBs contain similar one- and two-dimensional metallic bands independent of the width of the ReO_3-type slabs and distortions of WO_6 octahedra (*22*). Our recent study on the electrical and magnetic properties of $P_4W_8O_{32}$ single crystals (*21*), another member in the series, is in agreement with the theoretical prediction of Whangbo and coworkers (*22*).

Polycrystalline samples of two different polymorphs of PWO_5 were first reported by Kinomura *et al.* who also studied the electrical and magnetic properties in the high temperature region (*23*). According to their study, the low pressure form of PWO_5 crystallizes with monoclinic symmetry, which corresponds to $MPTB_p$ ($m = 2$), while the high pressure form is tetragonal. Both forms exhibited semiconducting behavior in the range of 77–420 K, although a higher conductivity was reported for the monoclinic form. The magnetization measurements in the range 77–500 K made on polycrystalline samples of both polymorphs revealed the existence of local magnetic moments. The infrared spectra of these two polymorphic forms of PWO_5 have also been reported recently (*24*).

Wang *et al.* have also prepared the second member of the $MPTB_p$; $(PO_2)_4(WO_3)_{2m}$, $m = 2$ or PWO_5 and determined its crystal structure with an orthorhombic unit cell (space group $Pna2_1$) (*10*). Their structural study showed that this compound contains chains or strings of corner sharing WO_6 octahedra along the *c*-axis (Fig. 1) that are isolated from each other by PO_4 tetrahedra.

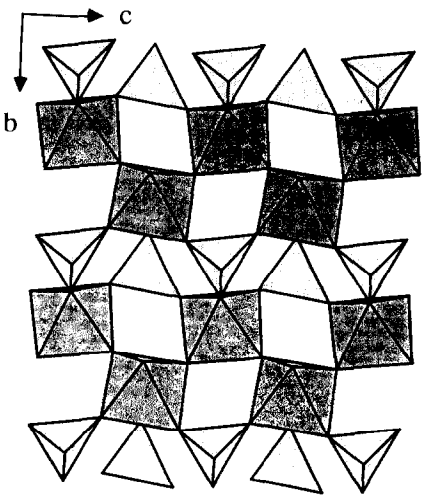

FIG. 1. PWO_5 crystal structure in the *b*–*c* plane showing corner sharing WO_6 octahedra chains.

The pentagonal tunnels, typical of the members of this series, are formed from corner sharing WO_6 and PO_4 polyhedra. Subsequent theoretical studies on the band electronic structure of this compound by Canadell and Whangbo suggested the presence of both localized and delocalized electrons in narrow and dispersive bands, respectively (*25*). They have predicted the compound to be metallic, and to exhibit an electronic instability arising from the delocalized electrons in the dispersive band. Furthermore, it was predicted that the presence of localized electrons in the narrow bands would provide a localized magnetic moment. Here we report results of our experimental studies on the magnetic and electronic transport properties of oriented single crystals of PWO_5.

II. Experimental

Dark-brown, plate-like crystals of PWO_5 were grown by reacting stoichiometric mixtures of P_2O_5 (Alfa products), WO_3 (Pura-

tronic, JMC Ltd.), and W (Alfa products) at 1200–1250°C for about 4 days in evacuated sealed quartz tubes. In a typical experiment, a quartz tube about 14 cm long and 1.0 cm in i.d. is charged with ~2.5 g of reactant mixture and inserted into a furnace horizontally such that a small temperature gradient of approximately 75°C is maintained along its length. The temperature of the furnace which was initially set at 600°C was slowly raised to 1200°C in about 6 hr.

Powder X-ray diffraction (PXD) patterns were recorded with a Scintag PAD V X-ray diffractometer using monochromatized Cu$K\alpha$ radiation. Silicon or Mica powder (NBS standard reference material 675) was used as an internal standard.

Electrical resistivity measurements on selected crystals (~2.0 mm × ~0.75 mm × ~0.20 mm) were made by a standard four-probe technique with a Displex cryostat (APD cryogenics, DE-202) in the temperature range of 50 to ~300 K. A two-probe technique was used to measure resistivity perpendicular to the plate of crystal due to its small dimension. The plate-like crystals selected were first washed with 5% HF at ~70°C for half an hour. Copper leads were then attached to the crystal under a microscope with silver paint. Alternatively, ultrasonically soldered indium contacts were first made on the crystals to which copper leads were attached with silver paint. Qualitative Seebeck measurements were made on single crystals by recording the variations in the potential drop under small applied thermal gradients.

The magnetic susceptibility on a batch of long plate-like crystals and on oriented single crystal were recorded with a Quantum Design SQUID magnetometer in the temperature range 2–300 K. The crystals selected were etched in 5% HF solution prior to measurement. The data were collected by first cooling the sample to 2 K and then applying a magnetic field of 5000 G. No corrections due to core diamagnetism were applied in the determination of susceptibility of the compound due to their negligible contributions, relative to the sample moment.

III. Results and Discussion

The product of the reaction for the growth of PWO_5 crystals used in this study almost always contains three different morphological forms of the compound. A polycrystalline sample mixed with some rounded crystals is obtained at the hot end of the quartz tube, while the long plate-like crystals are grown at the relatively cold end of the quartz tube. All the different forms of the compound are dark brown. At the completion of the reaction the quartz tube was always covered with a blue–black tint and a few long plate-like crystals were obtained in a typical experiment. Attempts to grow crystals of this phase by chemical vapor transport techniques using different transporting agents including KBr, KI, and $PtBr_2$ were not successful. The crystals obtained by this technique were either not suitable for physical measurements or of unknown phase.

The PXD patterns of the two different single crystal morphologies of PWO_5 are identical whereas the polycrystalline form contains some minor peaks due to impurities. Some of the peaks in the PXD patterns of the compound showed splitting which could not be accounted for by an orthorhombic unit cell. This implies that the actual symmetry of the compound may be lower than orthorhombic (*10*). The polycrystalline sample of the low pressure form of PWO_5 reported by Kinomura *et al.* could be indexed with a pseudo-orthorhombic cell although the true symmetry as determined from their single crystal study was monoclinic. Moreover, monoclinic symmetry with the β angle slightly different from 90° was implied by Wang *et al.* in their single-crystal study, where *hk*0 reflections with broad peak profiles suggested symmetry lower than orthorhombic (*10*). The observed

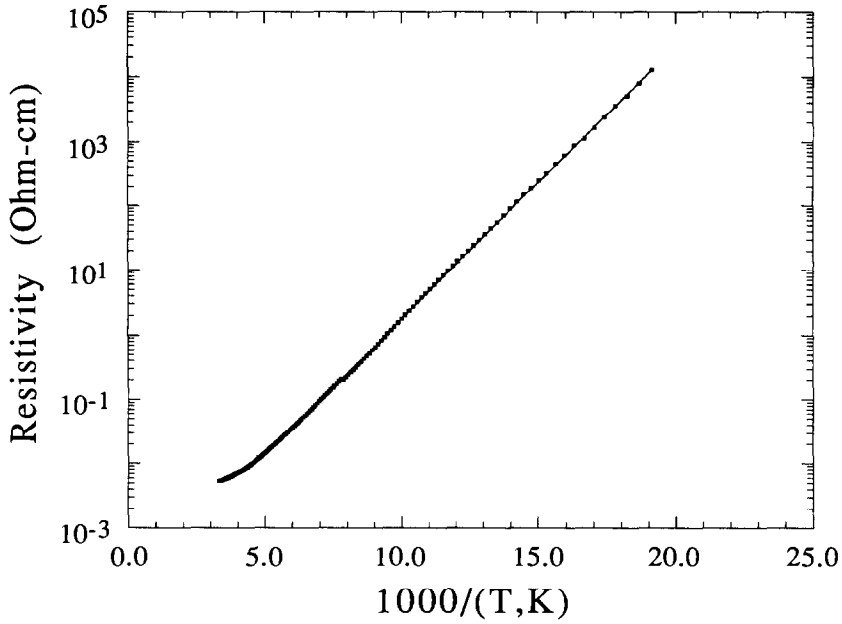

FIG. 2. Electrical resistivity as a function of inverse temperature along the longest axis of the plate of a single crystal.

PXD paterns of PWO_5 were indexed based on the orthorhombic unit cell (space group $Pna2_1$) as reported by Wang *et al.* The cell parameters evaluated from the least squares refinement of the observed *d*-spacings are: $a = 11.190(3)$ Å, $b = 6.557(2)$ Å, and $c = 5.226(1)$ Å.

Room temperature resistivity of a crystal measured along the long axis in the plane of the crystal (*c*-axis) is $5 \times 10^{-3}\ \Omega \cdot$ cm, while the resistivity measured along the short axis of the plate of the crystal (*b*-axis) is $4 \times 10^{-2}\ \Omega \cdot$ cm. The resistivity perpendicular to the plate of the crystal (*a*-axis), measured by a two-probe technique, is $\sim 1 \times 10^{-1}\ \Omega \cdot$ cm. Temperature dependence of the electrical resistivity (Fig. 2) shows semiconducting behavior from room temperature down to ~50 K. The sample also remains semiconducting up to 390 K. The resistivity below ~50 K is greater than $10^4\ \Omega \cdot$ cm, which is beyond the limit of our instrumentation and hence could not be recorded. The activation energy calculated for the low temperature region (~50–200 K), for the orientation of the crystal with highest conductivity, was 0.084 eV. Results of qualitative Seebeck measurements at room temperature show that the primary charge carriers are electrons (*n*-type).

The conductivity along the *c*-axis, the direction of the chains of corner sharing WO_6 octahedra, is about one and two orders magnitude higher than along the *b*- and *a*-axes, respectively. This observation is consistent with the structural properties which predict quasi one-dimensional electronic transport properties. The electronic band structure calculations performed on the basis of an orthorhombic unit cell indicated the presence of a dispersive band along the *c*-axis and narrow bands along the other crystallographic directions. Based on this model the conductivity along the *c*-axis should be the highest with metallic behavior. Although the conductivity is highest

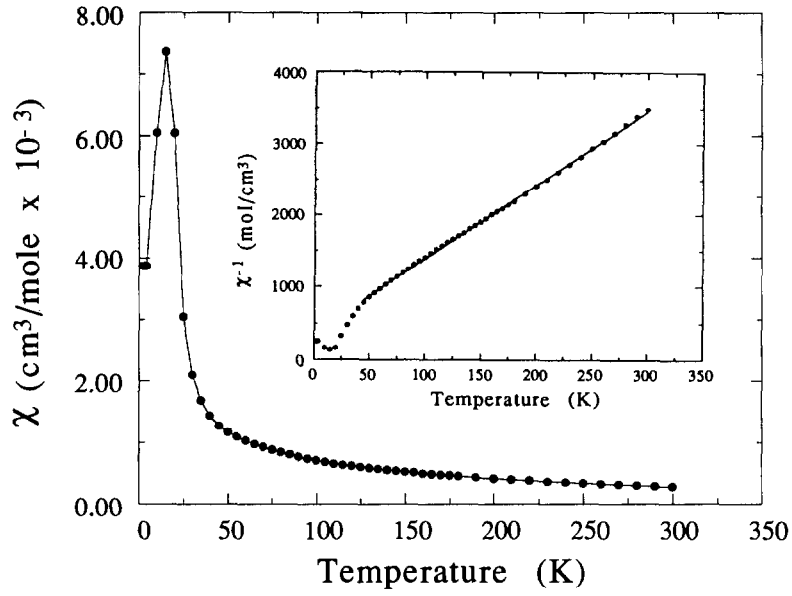

FIG. 3. Temperature dependence of magnetic susceptibility for a batch of PWO_5 crystals; inverse susceptibility as a function of temperature for the same plot (inset).

along the direction of the chains of WO_6 octahedra (c-axis), the observed semiconducting behavior is contrary to the metallic properties predicted by the theoretical calculation. These apparent discrepancies in the theoretical and observed electrical behavior of PWO_5 crystals may be due to subtle distortions of WO_6 octahedra.

Figure 3 illustrates the magnetic susceptibility of PWO_5 as a function of temperature measured on a batch of crystals whose long dimensions are oriented approximately perpendicular to the applied magnetic field. A well-defined maximum in the χ vs T plot near 15 K indicates the onset of antiferromagnetic ordering. The temperature dependence of the inverse susceptibility in the range 50–300 K follows Curie–Weiss behavior with $\theta = -34.6$ K. The effective magnetic moment in this temperature range is $0.88\,\mu_B$. A closer examination of the temperature-dependent inverse susceptibility (see inset Fig. 3) shows a significant deviation from linearity below ~50 K. This may indicate a change in the type of magnetic exchange interaction in this compound, possibly due to some type of structural phase transition. To further characterize the details of the magnetic ordering of the compound, similar measurements were made on a single crystal of PWO_5 along the three unique crystal axes relative to the applied magnetic field. Although the general trend in the magnetic susceptibilities along each crystal direction is similar, significant variations in the Néel temperatures are observed. The Néel temperatures measured along the short and long axes of the plate of the crystal (b- and c-axes) are ~16 K and 20 K, respectively. Figure 4 shows the temperature-dependent susceptibility measured along the c- and b-axes of the crystal. The sharp transition temperature at 20 K is reproducible and indicates the direction of highest electron–electron correlations in agreement with structural properties. The magnetic susceptibility measured perpendicular to the plate of the crystal (a-axis) is relatively

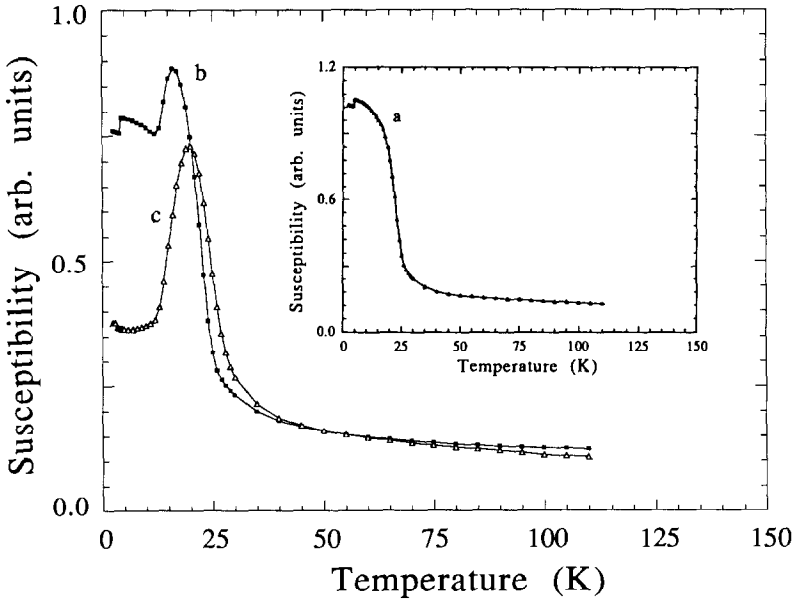

FIG. 4. Temperature dependence of magnetic susceptibility measured with applied magnetic field parallel to the short (square) and long (triangle) axes of the plate of a single crystal (*b*- and *c*-axes, respectively). Inset shows similar measurement but with applied magnetic field perpendicular to the plate of a single crystal (*a*-axis).

large compared to the other two directions and did not show a well-defined T_N. Instead, a plateau in the magnetization, a $\chi_{max} = 1.12 \times 10^{-2}$ cm^3/mole at 4.6 K is observed (Fig. 4, inset). We note that the low temperature behavior of the susceptibility, measured perpendicular to the crystal plate, shows slight variations in different measurements, probably due to difficulty in reproducing the orientation of the crystal relative to the applied magnetic field.

The PXD patterns of the crystals grown in our study suggest that the actual symmetry is lower than orthorhombic, in agreement with previous reports (*23*). This may account for the difference between observed electrical properties and that predicted by the theoretical calculations, which employed the orthorhombic model. PWO_5 shows semiconducting behavior down to ~50 K along all three crystal orientations, with high room temperature conductivity along the direction of the chains of corner sharing WO_6 octahedra. The low activation energy observed for the electron transport in PWO_5 is suggestive of small polaron hopping mechanism in narrow conduction bands derived from tungsten 5*d* and oxygen 2*p* orbitals. The sharp transition and high T_N in the magnetization measurement along the long axis of the plate of PWO_5 single crystal (*c*-axis) also suggests the presence of strong antiferromagnetic coupling of electrons relative to the other directions. Furthermore, the magnetization, with applied magnetic field parallel to this axis, is significantly lower than along other axes at low temperatures, consistent with the relatively high room temperature conductivity along this direction. The unusual electrical and magnetic properties observed in this compound compared to higher members in the

series is, perhaps, to be expected. Unlike in other known members of the MPTB family, there are no ReO_3-type slabs in PWO_5; the chains of corner sharing WO_6 octahedra are too isolated to allow delocalization of electrons along *a*- and *b*-axes.

We propose that the magnetic exchange interactions and semiconducting behavior observed in the present compound is related to charge disproportionation of W^{+5} to W^{+4} and W^{+6} states in PWO_5. This disproportionation may not be significant at higher temperature as indicated by the low room temperature resistivity, but renders the compound insulating at low temperatures. Indeed the observed deviation from linearity in the temperature-dependent inverse susceptibility at ~50 K may indicate this phenomenon to be responsible for a change in the type of magnetic exchange interaction, although some type of structural phase transition can not be ruled out. The magnetic moment of W^{+5} and W^{+4}, considering Russel–Saunders coupling scheme for tungsten ions, is 1.55 and 1.63 Bohr magnetons, respectively (*26, 27*). The magnetic moment of PWO_5 evaluated from the plot of χ^{-1} vs T is much lower (0.88 μ_B) than what would be expected for W^{+5}. However, the observed magnetic moment is about half that of what is expected for W^{+4}, and appears to be consistent with the disproportionation model proposed above.

IV. Conclusion

Plate-like single crystals of PWO_5 or $P_4W_4O_{20}$ were grown and their electrical and magnetic properties were investigated along the three unique crystallographic directions. This compound exhibits anisotropic electronic transport and magnetic properties. PWO_5 shows semiconducting behavior down to ~50 K along all three crystallographic axes with an activation energy of ~0.084 eV along the *c*-axis. Magnetization measurements indicate strong antiferromagnetic exchange interaction with T_N = 20 K along the *c*-axis of the crystal. Deviation from linearity in the temperature-dependent inverse susceptibility below ~50 K implies a change in the type of magnetic exchange interaction as a result of charge disproportionation of W^{+5} to W^{+4} and W^{+6} states. Moreover, this could account for the observed lowering of the structural symmetry by introducing distortions in the WO_6 octahedra. Among the known members of the MPTBp series, PWO_5 exhibits unique magnetic and electronic properties due to the isolated chains of WO_6 octahedra in the structure and exceptionally low oxidation state of tungsten. The apparent disagreement between the experimentally observed properties of PWO_5 and those predicted theoretically could be related to the distortions of the WO_6 octahedra. Finally, a charge density wave (CDW) instability cannot be completely ruled out. The high, room temperature conductivity (semimetallic) along the one-dimensional chains of WO_6 octahedra may suggest a transition to a metallic state at temperatures above 390 K due to a CDW instability as predicted by Whangbo and coworkers. However, more detailed studies of the crystal structure and further theoretical investigations may be necessary to explain these interesting physical properties of the compound.

Acknowledgments

We thank Professor J. H. Pifer and Professor W. H. McCarroll for their valuable suggestions. Helpful discussions with Dr. E. Wang, Dr. Li Shu, and Dr. R. Fuller are greatly appreciated. This work was supported by the National Science Foundation—Solid State Chemistry Grant DMR-87-14072.

References

1. E. WANG AND M. GREENBLATT, *J. Solid State Chem.* **76,** 340 (1988).
2. E. WANG, M. GREENBLATT, I. E.-I. RACHIDI, E.

CANADELL, AND M.-H. WHANGBO, *J. Solid State Chem.* **81,** 173 (1989).

3. E. WANG, M. GREENBLATT, I. E.-I. RACHIDI, E. CANADELL, AND M.-H. WHANGBO, *Inorg. Chem.* **28,** 2451 (1989).
4. (*a*) E. WANG, M. GREENBLATT, I. E.-I. RACHIDI, E. CANADELL, M.-H. WHANGBO, AND S. VADLAMANNATI, *Phys. Rev. B* **39,** 12,969 (1989); (*b*) E. WANG, M. GREENBLATT, I. E.-I. RACHIDI, E. CANADELL, M.-H. WHANGBO, AND S. VADLAMANNATI, *Phys. Rev. B* **40,** 11,964 (1989).
5. E. WANG, M. GREENBLATT, I. E.-I. RACHIDI, E. CANADELL AND M.-H. WHANGBO, *J. Solid State Chem.* **80,** 266 (1989).
6. P. FOURY, J. P. POUGET, E. WANG, AND M. GREENBLATT, *Synthetic Metals* **43,** 3973 (1991).
7. P. FOURY, J. P. POUGET, E. WANG, AND M. GREENBLATT, *Europhysics Letters,* to appear.
8. J. P. GIROULT, M. GOREAUD, PH. LABBÉ, AND B. RAVEAU, *Acta Crystallogr. Sect. B* **37,** 2139 (1981).
9. PH. LABBE, M. GOREAUD, AND B, RAVEAU, *J. Solid State Chem.* **61,** 324 (1986).
10. S. L. WANG, C. C. WANG, AND K. H. LII, *J. Solid State Chem.* **82,** 298 (1989).
11. A. BENMOUSSA, PH. LABBÉ, D. GROULT, AND B. RAVEAU, *J. Solid State Chem.* **44,** 318 (1982).
12. B. DOMENGÉS, M. GOREAUD, PH. LABBÉ, AND B. RAVEAU, *Acta Crystallogr. Sect. B* **38,** 1724 (1982).
13. B. DOMENGÉS, F. STUDER, AND B. RAVEAU, *Mater. Res. Bull.* **18,** 669 (1983).
14. B. DOMENGÉS, M. HERVIEU, B. RAVEAU, AND R. J. D. TILLEY, *J. Solid State Chem.* **54,** 10 (1984).
15. A. BENMOUSSA, D. GROULT, PH. LABBÉ, AND B. RAVEAU, *Acta Crystallogr. Sect. C* **40,** 573 (1984).
16. M. LAMIRE, PH. LABBE, M. GOREAUD, AND B. RAVEAU, *J. Solid State Chem.* **66,** 64 (1987).
17. J. P. GIROULT, M. GOREAUD, PH. LABBÉ, AND B. RAVEAU, *J. Solid State Chem.* **44,** 407 (1982).
18. B. DOMENGÉS, M. HERVIEU, B. RAVEAU, AND M. O'KEEFFE, *J. Solid State Chem.* **72,** 155 (1988).
19. A. BENMOUSSA, D. GROULT, AND B. RAVEAU, *Rev. Chim. Miner.* **21,** 710 (1984).
20. B. DOMENGES, M. GOREAUD, PH. LABBÉ, AND B. RAVEAU, *J. Solid State Chem.* **50,**173 (1983).
21. Z. S. TEWELDEMEDHIN, K. V. RAMANUJACHARY, AND M. GREENBLATT, to be published.
22. (*a*) E. Canadell, M.-H. Whangbo, and I. E.-I. Rachidi, *Inorg. Chem.* **29,** 3871, (1990); (*b*) E. Canadell and M.-H. Whangbo, *Phys. Rev. B* **43,**1894 (1991).
23. N. KINOMURA, M. HIROSE, N. KUMADA, F. MUTO, AND T. ASHIDA, *J. Solid State Chem.* **77,** 156 (1988).
24. E. J. BARAN, I. L. BOTTO, N. KINOMUIRA, AND N. KUMADA, *J. Solid State Chem.* **89,** 144 (1990).
25. E. CANADELL, AND M.-H. WHANGBO, *J. Solid State Chem.* **86,** 131 (1990).
26. L. E. CONROY AND M. J. SIENKO, *J. Am. Chem. Soc.***74,** 3520 (1952).
27. J. P. GIROULT, M. GOREAUD, PH. LABBÉ, J. PROVOST, AND B. RAVEAU, *Mater. Res. Bull.* **16,** 811 (1981).